JACS
JOURNAL OF THE AMERICAN CHEMICAL SOCIETY
Communication
pubs.acs.org/JACS

# A Mixed-Crystal Lanthanide Zeolite-like Metal–Organic Framework as a Fluorescent Indicator for Lysophosphatidic Acid, a Cancer Biomarker

Shi-Yuan Zhang,[†,‡] Wei Shi,*[,†] Peng Cheng,[†] and Michael J. Zaworotko*[,‡]

[†]Department of Chemistry, Key Laboratory of Advanced Energy Materials Chemistry (MOE), Collaborative Innovation Center of Chemical Science and Engineering, Nankai University, Tianjin 300071, P. R. China

[‡]Department of Chemical & Environmental Science and Materials and Surface Science Institute, University of Limerick, Limerick, Republic of Ireland

Supporting Information

**ABSTRACT:** Two lanthanide zeolite-like metal–organic frameworks (Ln-ZMOFs) with **rho** topology, **Tb-ZMOF** and **Eu-ZMOF**, were constructed by self-assembly of a 4-connected lanthanide molecular building block and a bipyridine-dicarboxylate ligand. Varying the $Tb^{3+}$ and $Eu^{3+}$ ratio during synthesis afforded three mixed-crystal isostructural **MZMOFs** with variable Eu:Tb stoichiometry. Fluorescence studies revealed that a methanol suspension of one of these mixed crystals, **MZMOF-3**, exhibits selective detection of lysophosphatidic acid (LPA), a biomarker for ovarian cancer and other gynecologic cancers. Linear correlation between the integrated fluorescence intensity and the concentration of LPA was observed, enabling quantitative analysis of LPA in physiologically relevant ranges (1.4–43.3 $\mu$M). **MZMOF-3** therefore has the potential to act as a self-referencing and self-calibrating fluorescent indicator for LPA.

Ovarian cancer has the lowest survival rate of all gynecologic malignancies, largely because late diagnosis mitigates against effective therapeutics.[1] Lysophosphatidic acid (LPA, Scheme 1), a bioactive phospholipid, exhibits pleiomorphic functions in multiple cell lineages and stimulates the proliferation of cancer cells. Accompanied by a complicated cascade of genetic, molecular, and biochemical events, LPA levels are consistently elevated in plasma, suggesting that LPA plays a role in the pathophysiology of ovarian cancer.[2] Moreover, increased levels of LPA, altered receptor expression in ovarian carcinogenesis, and metastasis demonstrate markedly different responses to LPA than most other epithelial tumors. Therefore, the rapid detection of plasma LPA levels could represent a promising approach to diagnose this devastating disease during its early stages. However, the selective and sensitive detection of LPA is currently limited due to expensive, sophisticated devices and complicated procedures, including tandem mass spectroscopy, capillary electrophoresis, and radio-enzymatic assays.[3] Fluorometric techniques could offer facile, sensitive, and fast assays and would likely be preferred if available. We address this matter herein through the study of a family of isostructural lanthanide metal–organic frameworks (Ln-MOFs).

**Scheme 1. Structures of LPA and GPA**

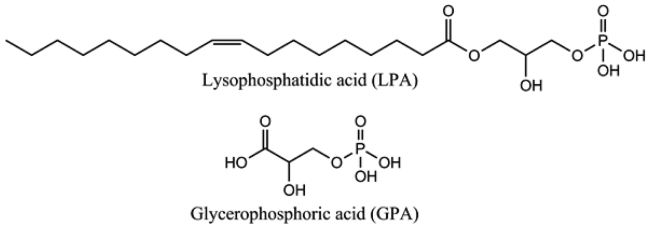


MOFs, or porous coordination polymers,[4] have attracted great attention for their high permanent porosity coupled with structural tunability; hence, they show potential for utility in hydrogen storage,[5] gas separation,[6] enhanced catalysis,[7] smart sensors,[8] and drug delivery.[9] Ln-MOFs offer the possibility of exploiting the luminescence properties of lanthanide cations such as long emission lifetimes with sharp and characteristic line emissions.[10] In addition, the luminescence intensity of Ln-MOFs can be tuned by the host–guest chemistry, thereby providing an opportunity for chemical sensing of molecules such as LPA.

Ln-MOFs with zeolite-like topologies can exhibit high porosity, stability, and tunable composition. Large pore diameters and high specific pore volume enable guest molecules, even relatively large molecules like LPA, to interact with the host framework. Although zeolite-like MOFs (ZMOFs) are already known for transition metals,[11] lanthanide ZMOFs (Ln-ZMOFs) are understudied, presumably because their high coordination numbers and diverse coordination environments make it difficult to design suitable 4-connected nodes. We herein demonstrate that judicious selection of luminescent $Ln^{3+}$ centers and ligands to form secondary building units (SBUs)[12] enables construction of a family of Ln-ZMOFs with zeolitic topology. Specifically, tetrahedral building units (TBUs), made by reacting 2,2′-bipyridine-6,6′-dicarboxylic acid ($H_2$bpdc) with $Tb(NO_3)_3 \cdot 6H_2O$ in methanol/chloroform at 80 °C, afford colorless polyhedral crystals of $[Tb_{48}(NO_3)_{48}(bpdc)_{48}]\cdot G_x$ (**Tb-ZMOF**; G = guest) with **rho** topology. **Eu-ZMOF** was obtained using the same procedure using by $Eu(NO_3)_3 \cdot 6H_2O$. Mixed-crystal variants $Eu_xTb_{1-x}$-ZMOF were synthesized by varying the $Eu^{3+}$:$Tb^{3+}$ stoichiometry.

**Received:** July 3, 2015
**Published:** September 10, 2015




DOI: 10.1021/jacs.5b06929
J. Am. Chem. Soc. 2015, 137, 12203–12206

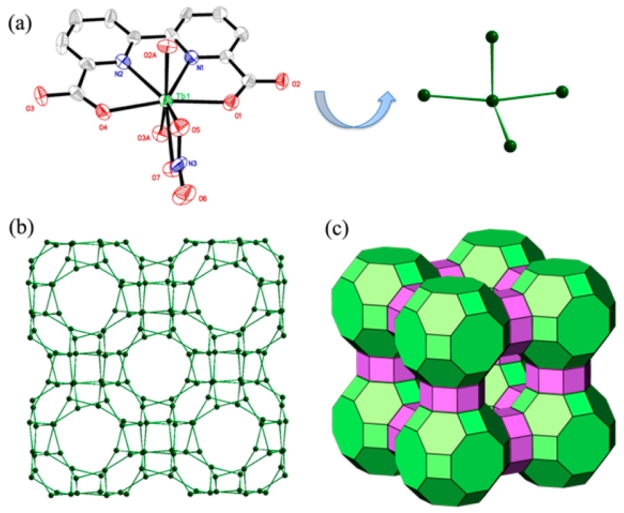


**Figure 1.** Crystal structure of **Tb-ZMOF**: (a) the eight-coordinated $Tb^{3+}$ SBU that serves as a 4-connected node; (b) perspective view of the $\alpha$- and $\beta$-cages in Tb-ZMOF (green dots correspond to $Tb^{3+}$ ions; green lines represent carboxylate moieties); and (c) tiling representation of the **rho** topology of **Tb-ZMOF**.

Single-crystal X-ray diffraction analysis reveals that **Tb-ZMOF** crystallizes in the cubic space group $Pn\bar{3}n$. There is one crystallographically independent $Tb^{3+}$ ion, which is coordinated by two nitrogen atoms from one $bpdc^{2-}$, four oxygen atoms from three other $bpdc^{2-}$ ligands, and two oxygen atoms from a nitrate ion. Each $bpdc^{2-}$ anion acts as both a linker and a chelator and coordinates to three $Tb^{3+}$ ions. The eight-coordinate $Tb^{3+}$ complex, thereby generated, serves as a TBU, as shown in Figure 1a. Self-assembly of these TBUs affords truncated cuboctahedral cages ($\alpha$-cages), which when further linked through double-eight-membered rings generate $\beta$-cages and a **rho** topology MOF (Figure 1b). Unlike previous **rho** ZMOFs, carboxylate groups instead of nitrogen donors direct the framework topology. Tb−N bonds serve an ancillary role by completing the eight-coordinate geometry. ZMOFs that exhibit **rho** topology have been observed for $Zn^{2+}$,[11a,13] $Cd^{2+}$,[11d] and $In^{3+}$.[14] To our knowledge, **Tb-ZMOF** represents the first example of a zeolite-like lanthanide MOF with **rho** topology. Given that a TBU of **Tb-ZMOF** is 8 times larger than that of zeolite **rho**, the $\alpha$-cage is 17.6 Å in diameter. The packing of the $\alpha$- and $\beta$-cages is evident from a tiling illustration (Figure 1c). The solvent-accessible volume of **1** is 37.5% when calculated using PLATON.[15]

Varying the molar ratio of $Tb^{3+}$ and $Eu^{3+}$ resulted in mixed-crystal variants $Eu_xTb_{1-x}$-ZMOF:$Eu_{0.2206}Tb_{0.7794}$-ZMOF (**MZMOF-1**), $Eu_{0.3525}Tb_{0.6415}$-ZMOF (**MZMOF-2**), and $Eu_{0.6059}Tb_{0.3941}$-ZMOF (**MZMOF-3**), as determined by inductively coupled plasma atomic emission spectroscopy. As expected, each framework is isostructural with **Tb-ZMOF** according to powder X-ray diffractograms (Figure S1). The void spaces of **Tb-ZMOF**, **Eu-ZMOF**, and the **MZMOFs** are occupied by guest molecules which can be removed by heating (Figure S2). Thermogravimetry curves showed an initial weight loss on going from 25 to 170 °C, corresponding to the release of guest molecules. No clear weight loss was observed between 170 and 410 °C, indicating a high degree of thermal stability.

The photoluminescence spectra of **Tb-ZMOF**, **Eu-ZMOF**, and the **MZMOFs** suspended in methanol were collected in the 450−700 nm range with excitation at 300 nm (Figure 2). The characteristic lanthanide luminescence was observed with sharp

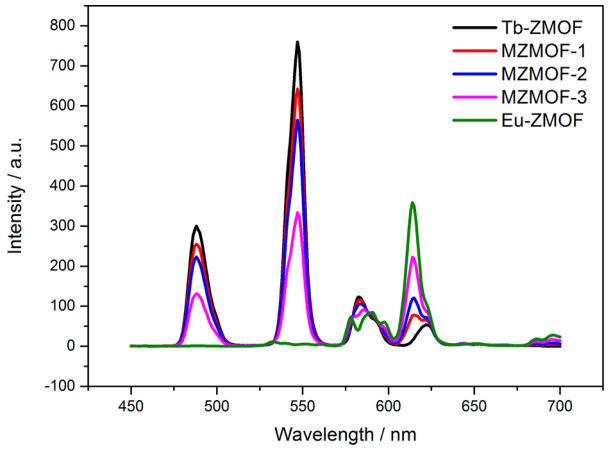


**Figure 2.** Relative luminescence intensity changes of **Tb-ZMOF**, **Eu-ZMOF**, and the **MZMOFs** suspended in MeOH. The emission spectra were recorded from 450 to 700 nm upon 300 nm excitation.

and well-resolved emission peaks. **Tb-ZMOF** displays emission bands at 488, 546, 583, and 621 nm in the visible region, coming from the $^5D_4 \rightarrow {}^7F_J$ ($J$ = 6, 5, 4, and 3) transitions of $Tb^{3+}$ ions. Characteristic transitions of the $Eu^{3+}$ ions ascribed to $^5D_0 \rightarrow {}^7F_J$ ($J$ = 1, 2, and 3) transitions are evident for **Eu-ZMOF** at 589, 616, and 653 nm. As expected, **MZMOFs** simultaneously produce the characteristic emission bands of both $Tb^{3+}$ and $Eu^{3+}$ ions, and their respective emission intensities decrease and increase as composition varies. Therefore, we have modulated the fluorescence performance of the individual lanthanide ions by controlling the ratio of the two metals during synthesis.

In order to establish the performance of **Tb-ZMOF**, **Eu-ZMOF**, and the three **MZMOFs** toward LPA, the fluorescent emission responses were collected using an LPA solution in MeOH. Specifically, the fluorescence spectrum of each material suspended in MeOH (2 mL) was recorded, to this was added a 0.05 mM solution of LPA (0.5 and 1 mL), and the resulting emissions were monitored. The intensities of the $^5D_4 \rightarrow {}^7F_5$ ($I_{Tb}$ = 546 nm) and $^5D_0 \rightarrow {}^7F_2$ ($I_{Eu}$ = 613 nm) transitions were used for the calculation of intensity change by $(I - I_0)/I_0$, where $I_0$ is the initial fluorescence intensity before the addition of analyte and $I$ is the fluorescence intensity in the presence of analyte. As shown in Figures 3 and S3−S7, the emission intensities of **Tb-ZMOF** suspensions decrease gradually upon incremental addition of LPA (0.05 mM). In contrast, fluorescence enhancement of **Eu-ZMOF** suspensions was observed: an 8% increase vs the initial fluorescence intensity. Further addition of LPA led to a lower enhancement of fluorescence intensity, which was most pronounced in dilute **Eu-ZMOF** suspensions. Mixed-crystal **MZMOFs** exhibited behavior similar to that of **Tb-ZMOF** and **Eu-ZMOF**. The intensity ratio of $Eu^{3+}$ and $Tb^{3+}$ (integrated intensity, $I = I_{Eu}/I_{Tb}$) correlated well with the concentration of LPA. It was found that the best sensitivity toward LPA was exhibited by **MZMOF-3**: 82% enhancement of integrated intensity.

Compounds present in blood plasma might interfere with detection of LPA. In order to mimic blood plasma, water, glucose (4.5−5.5 mM), $Na^+$ (136−146 mM), $Cl^-$ (96−106 mM), L-proline (3−5 mM), and urea (3.5−7.0 mM) were prepared as MeOH solutions. The luminescence intensities of **Tb-ZMOF**, **Eu-ZMOF**, and **MZMOF** suspensions in the presence of upper limit concentrations of these major plasma components were determined (Figures 3 and S3−S7). For **Tb-ZMOF** and **Eu-**


DOI: 10.1021/jacs.5b06929
J. Am. Chem. Soc. 2015, 137, 12203−12206

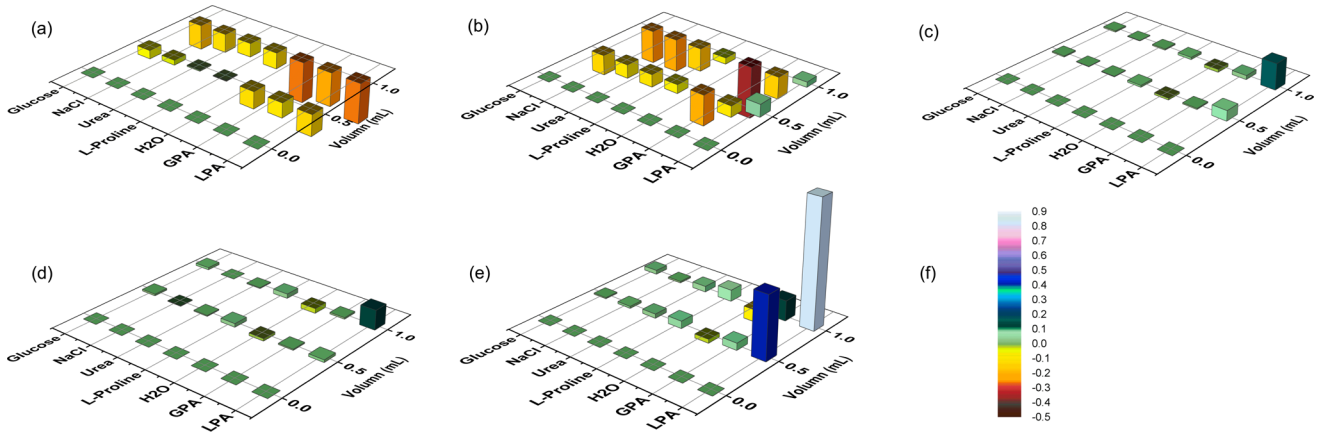


**Figure 3.** Relative luminescence intensity changes of (a) **Tb-ZMOF**, (b) **Eu-ZMOF**, (c) **MZMOF-1** (d) **MZMOF-2**, and (e) **MZMOF-3** in the presence of different analytes. All materials were suspended in MeOH at 0.3 mg/mL. The concentrations of LPA, GPA, L-proline, urea, NaCl, and glucose were 0.05, 0.05, 5, 7, 146, and 5.5 mM, respectively. $H_2O$ was used pure. Fluorescent emission was monitored by the characteristic transitions of the $Tb^{3+}$ ions at 546 nm ($I_{Tb}$) and the $Eu^{3+}$ ions at 616 nm ($I_{Eu}$) when excited at 300 nm. The intensity change is indicated by the colormap from −0.5 to 0.9 (f).

**ZMOF**, these additives were found to exhibit different behaviors, but in general they exhibit fluorescent emission signals comparable to that of LPA. However, **MZMOFs** were found to exhibit different selectivity for LPA over the other analytes. There were negligible effects on fluorescence intensity with **MZMOF-1** and **MZMOF-2** suspensions. Slightly increased relative luminescence intensities were observed in **MZMOF-3** when compared to **MZMOF-1** and **MZMOF-2**, but with 10−80 times lower response than that of LPA. Fluorescence titration of different concentrations of LPA in the presence of a mixture of L-proline (5 mM), urea (7 mM), NaCl (146 mM), and glucose (5.5 mM) was also studied (Figures S14−S16). The observed intensities were lower (ca. 30%) than that of pure LPA, but, nevertheless, a good linear relationship was retained (Figure S17).

Physiological concentrations of LPA in plasma typically vary from 0.1 to 6.3 $\mu$M, whereas danger levels for ovarian cancer are indicated by concentrations on the order of 43.1 $\mu$M.[2] In order to investigate the performance of **MZMOF-3** for detecting LPA within that range, fluorescence intensity was monitored upon incremental addition (0.1 mL) of 0.05 mM LPA solution (Figure S9). The fluorescence titration results are visualized by plotting the integrated fluorescence intensity versus real-time concentration of LPA in **MZMOF-3** suspension (Figure S12b). The plot reveals that there is a linear relationship with a slope of 0.05010 ± 0.00179, indicating that **MZMOF-3** is a self-referencing fluorescent sensor. Fluorescence titrations were also performed with 0.03, 0.10, and 0.13 mM LPA (Figures S8, S10, and S11, respectively). The integrated intensity was observed to linearly correlate to the concentration of LPA (Figure S12). Indeed, the slopes obtained from each curve are indistinguishable. Furthermore, four individual measurements were integrated into one complete plot with a slope of 0.04852 ± 0.00051, as shown in Figures 4 and S12e. Accordingly, fluorescence intensity from LPA in **MZMOF-3** suspension is quantitive in the concentration range from 1.4 to 43.3 $\mu$M, which reflects typical physiological levels. Further, the data indicate that intensity is independent of the amount of **MZMOF-3**, the only correlation being to LPA concentration. **MZMOF-3** is therefore a self-calibrating fluorescent indicator and does not require additional calibration of luminescence intensity.

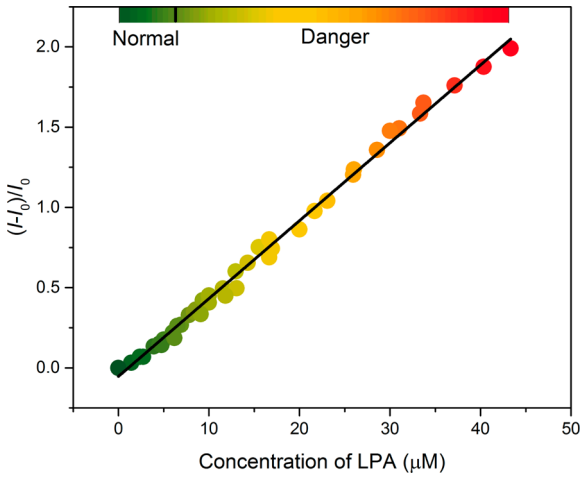


**Figure 4.** Integrated luminescence intensity changes of **MZMOF-3** suspended in MeOH toward 0.03, 0.10, and 0.13 mM LPA.

The fluorescence response of **MZMOF-3** in water (0.3 mg/mL water suspension) upon addition of LPA (0.10 mM aqueous solution) was also studied. Negligible effect on integrated fluorescence intensity was observed (Figure S13). This could be the result of competition with water for binding sites within **MZMOF-3** or aggregation of LPA to form micelles. However, lyophilized plasma reconstituted by MeOH would represent a viable approach to LPA detection.

The fluorescent emission properties of **MZMOF-3** with respect to LPA suggest an energy-transfer mechanism; i.e., the increased intensity of $Eu^{3+}$ transitions and the decreased intensity of $Tb^{3+}$ transitions induced by energy transfer from $Tb^{3+}$ to $Eu^{3+}$ ions were significantly enhanced in the presence of LPA. To address this matter, the lifetime of **MZMOF-3** toward LPA was monitored at 546 and 613 nm (Figure S18). The fluorescent lifetime of $^5D_4$ ($\tau_{Tb}$) is reduced by the addition of LPA (0.5−1 mL), whereas the $^5D_0 \rightarrow {}^7F_2$ ($\tau_{Eu}$) lifetime increases (Table S2). This is consistent with an energy-transfer mechanism from $Tb^{3+}$ to $Eu^{3+}$ ions in the presence of LPA. On the contrary, the lifetimes of both cations in **MZMOF-1** and **MZMOF-2** increase as LPA is added. The effect of LPA is consistent with intermolecular interactions between LPA and **MZMOF-3**.


DOI: 10.1021/jacs.5b06929
J. Am. Chem. Soc. 2015, 137, 12203−12206

Notably, LPA and GPA have the same head phosphate and 2-*sn*-OH functional groups but very different end groups (Scheme 1), yet they exhibit different fluorescence behavior toward **MZ-MOF-3** (Figure 3). We presume that the oleoyl acid chain in combination with the phosphate of LPA generates different hydrogen-bonding and/or hydrophobic interactions, which might account for the magnitude of its luminescence intensity and its affinity toward **MZMOF-3**.

In conclusion, we report a single-step synthesis of lanthanide zeolite-like metal−organic frameworks, **Tb-ZMOF** and **Eu-ZMOF**, which are based upon 4-connected single-lanthanide-ion-based TBUs. Isostructural mixed-crystal **MZMOFs** prepared by varying the molar ratios of $Tb^{3+}$ to $Eu^{3+}$ exhibit the characteristic emission bands of both $Tb^{3+}$ and $Eu^{3+}$ ions. **MZMOF-3** was found to exhibit selective detection of LPA, which is a biomarker of ovarian cancer, even in the presence of major components of blood plasma. To our knowledge, this is the first example of a MOF that senses trace amounts of LPA at biologically relevant concentrations. **MZMOF-3** not only exhibits high sensitivity and selectivity to LPA but also is self-referencing and self-calibrating. These results suggest a new general route to create luminescent mixed-crystal Ln-MOFs that might enable early detection of disease or be suitable for other biochemical sensing applications.

## ■ ASSOCIATED CONTENT

### Supporting Information

The Supporting Information is available free of charge on the ACS Publications website at DOI: 10.1021/jacs.5b06929.

Experimental details and characterization data (PDF)
X-ray crystallographic data for **Tb-ZMOF** (CIF)

## ■ AUTHOR INFORMATION


### Corresponding Authors

*shiwei@nankai.edu.cn
*xtal@ul.ie


### Notes

The authors declare no competing financial interest.

## ■ ACKNOWLEDGMENTS

This work was supported by MOST (973 program, 2012CB821702), NSFC (21373115, 21331003 and 91422302) and 111 Project (B12015). We also acknowledge Science Foundation of Ireland (13/RP/B2549).

## ■ REFERENCES


(1) (a) Chobanian, N.; Dietrich, C. S. *Surg. Clin. North Am.* **2008**, *88*, 285. (b) Jemal, A.; Siegel, R.; Xu, J.; Ward, E. *Ca-Cancer J. Clin.* **2010**, *60*, 277.

(2) (a) Mills, G. B.; Moolenaar, W. H. *Nat. Rev. Cancer* **2003**, *3*, 582. (b) Xu, Y.; Shen, Z.; Wiper, D. W.; Wu, M.; Morton, R. E.; Elson, P.; Kennedy, A. W.; Belinson, J.; Markman, M.; Casey, G. *J. Am. Med. Assoc.* **1998**, *280*, 719. (c) Umezu-Goto, M.; Tanyi, J.; Lahad, J.; Liu, S.; Yu, S.; Lapushin, R.; Hasegawa, Y.; Lu, Y.; Trost, R.; Bevers, T.; Jonasch, E.; Aldape, K.; Liu, J.; James, R. D.; Ferguson, C. G.; Xu, Y.; Prestwich, G. D.; Mills, G. B. *J. Cell. Biochem.* **2004**, *92*, 1115. (d) Ren, J.; Xiao, Y. J.; Singh, L. S.; Zhao, X.; Zhao, Z.; Feng, L.; Rose, T. M.; Prestwich, G. D.; Xu, Y. *Cancer Res.* **2006**, *66*, 3006. (e) Sutphen, R.; Xu, Y.; Wilbanks, G. D.; Fiorica, J.; Grendys, E. C.; LaPolla, J. P.; Arango, H.; Hoffman, M. S.; Martino, M.; Wakeley, K.; Griffin, D.; Blanco, R. W.; Cantor, A. B.; Xiao, Y. J.; Krischer, J. P. *Cancer Epidemiol. Biomark. Prev.* **2004**, *13*, 1185.

(3) (a) Kim, H.; Yoon, H.-R.; Pyo, D. *Bull. Korean Chem. Soc.* **2002**, *23*, 1139. (b) Saulnier-Blache, J. S.; Girard, A.; Simon, M.-F.; Lafontan, M.; Valet, P. *J. Lipid Res.* **2000**, *41*, 1947. (c) Tigyi, G.; Miledi, R. *J. Biol. Chem.* **1992**, *267*, 21360. (d) Shen, Z.; Wu, M.; Elson, P.; Kennedy, A. W.; Belinson, J.; Casey, G.; Xu, Y. *Gynecol. Oncol.* **2001**, *83*, 25.

(4) (a) Batten, S. R.; Neville, S. M.; Turner, D. R. *Coordination Polymers: Design, Analysis and Application*; Royal Society of Chemistry: Cambridge, U.K., 2009. (b) MacGillivray, L. R. *Metal−Organic Frameworks: Design and Application*; John Wiley & Sons: Hoboken, NJ, 2010. (c) Moulton, B.; Zaworotko, M. J. *Chem. Rev.* **2001**, *101*, 1629. (d) Kitagawa, S.; Kitaura, R.; Noro, S.-i. *Angew. Chem., Int. Ed.* **2004**, *43*, 2334.

(5) (a) Murray, L. J.; Dincă, M.; Long, J. R. *Chem. Soc. Rev.* **2009**, *38*, 1294. (b) Yang, S.; Lin, X.; Blake, A. J.; Walker, G. S.; Hubberstey, P.; Champness, N. R.; Schröder, M. *Nat. Chem.* **2009**, *1*, 487.

(6) (a) Li, J.-R.; Kuppler, R. J.; Zhou, H.-C. *Chem. Soc. Rev.* **2009**, *38*, 1477. (b) Nugent, P.; Belmabkhout, Y.; Burd, S. D.; Cairns, A. J.; Luebke, R.; Forrest, K.; Pham, T.; Ma, S.; Space, B.; Wojtas, L.; Eddaoudi, M.; Zaworotko, M. J. *Nature* **2013**, *495*, 80. (c) Dybtsev, D. N.; Chun, H.; Yoon, S. H.; Kim, D.; Kim, K. *J. Am. Chem. Soc.* **2004**, *126*, 32. (d) Sumida, K.; Rogow, D. L.; Mason, J. A.; McDonald, T. M.; Bloch, E. D.; Herm, Z. R.; Bae, T. H.; Long, J. R. *Chem. Rev.* **2012**, *112*, 724.

(7) (a) Wang, Z.; Chen, G.; Ding, K. *Chem. Rev.* **2009**, *109*, 322. (b) Corma, A.; Garcia, H.; Llabres i Xamena, F. X. *Chem. Rev.* **2010**, *110*, 4606. (c) Lee, J.; Farha, O. K.; Roberts, J.; Scheidt, K. A.; Nguyen, S. T.; Hupp, J. T. *Chem. Soc. Rev.* **2009**, *38*, 1450. (d) Ma, L.; Abney, C.; Lin, W. *Chem. Soc. Rev.* **2009**, *38*, 1248.

(8) (a) Chen, B.; Xiang, S.; Qian, G. *Acc. Chem. Res.* **2010**, *43*, 1115. (b) Chen, B.; Wang, L.; Zapata, F.; Qian, G.; Lobkovsky, E. B. *J. Am. Chem. Soc.* **2008**, *130*, 6718. (c) Cui, Y.; Xu, H.; Yue, Y.; Guo, Z.; Yu, J.; Chen, Z.; Gao, J.; Yang, Y.; Qian, G.; Chen, B. *J. Am. Chem. Soc.* **2012**, *134*, 3979.

(9) (a) Vallet-Regí, M.; Balas, F.; Arcos, D. *Angew. Chem., Int. Ed.* **2007**, *46*, 7548. (b) Horcajada, P.; Chalati, T.; Serre, C.; Gillet, B.; Sebrie, C.; Baati, T.; Eubank, J. F.; Heurtaux, D.; Clayette, P.; Kreuz, C.; Chang, J. S.; Hwang, Y. K.; Marsaud, V.; Bories, P. N.; Cynober, L.; Gil, S.; Ferey, G.; Couvreur, P.; Gref, R. *Nat. Mater.* **2010**, *9*, 172.

(10) (a) Cui, Y.; Chen, B.; Qian, G. *Coord. Chem. Rev.* **2014**, *273-274*, 76. (b) Sava, D. F.; Rohwer, L. E. S.; Rodriguez, M. A.; Nenoff, T. M. *J. Am. Chem. Soc.* **2012**, *134*, 3983. (c) Takashima, Y.; Martinez, V. M.; Furukawa, S.; Kondo, M.; Shimomura, S.; Uehara, H.; Nakahama, M.; Sugimoto, K.; Kitagawa, S. *Nat. Commun.* **2011**, *2*, 168. (d) Bünzli, J.-C. G. *Chem. Rev.* **2010**, *110*, 2729. (e) Cheng, P. *Lanthanide Metal-Organic Frameworks*; Springer: Berlin, 2015. (f) Choppin, G. R.; Peterman, D. R. *Coord. Chem. Rev.* **1998**, *174*, 283. (g) Handl, H. L.; Gillies, R. J. *Life Sci.* **2005**, *77*, 361. (k) Li, H. H.; Shi, W.; Zhao, K. N.; Niu, Z.; Li, H. M.; Cheng, P. *Chem. - Eur. J.* **2013**, *19*, 3358. (l) Zhou, J. M.; Shi, W.; Xu, N.; Cheng, P. *Inorg. Chem.* **2013**, *52*, 8082.

(11) (a) Huang, X.-C.; Lin, Y.-Y.; Zhang, J.-P.; Chen, X.-M. *Angew. Chem., Int. Ed.* **2006**, *45*, 1557. (b) Park, K. S.; Ni, Z.; Côté, A. P.; Choi, J. Y.; Huang, R.; Uribe-Romo, F. J.; Chae, H. K.; O'Keeffe, M.; Yaghi, O. M. *Proc. Natl. Acad. Sci. U. S. A.* **2006**, *103*, 10186. (c) Liu, Y.; Kravtsov, V. Ch.; Larsen, R.; Eddaoudi, M. *Chem. Commun.* **2006**, 1488. (d) Sava, D. F.; Kravtsov, V. Ch.; Nouar, F.; Wojtas, L.; Eubank, J. F.; Eddaoudi, M. *J. Am. Chem. Soc.* **2008**, *130*, 3768. (e) Zhang, J.; Wu, T.; Zhou, C.; Chen, S.; Feng, P.; Bu, X. *Angew. Chem., Int. Ed.* **2009**, *48*, 2542. (f) Zheng, S.; Wu, T.; Zhang, J.; Chow, M.; Nieto, R. A.; Feng, P.; Bu, X. *Angew. Chem., Int. Ed.* **2010**, *49*, 5362. (g) Eddaoudi, M.; Sava, D. F.; Eubank, J. F.; Adil, K.; Guillerm, V. *Chem. Soc. Rev.* **2015**, *44*, 228.

(12) (a) Tranchemontagne, D. J.; Mendoza-Cortes, J. L.; O'Keeffe, M.; Yaghi, O. M. *Chem. Soc. Rev.* **2009**, *38*, 1257. (b) Perry, J. J.; Perman, J. A.; Zaworotko, M. J. *Chem. Soc. Rev.* **2009**, *38*, 1400.

(13) (a) Banerjee, R.; Phan, A.; Wang, B.; Knobler, C.; Furukawa, H.; O'Keeffe, M.; Yaghi, O. M. *Science* **2008**, *319*, 939. (b) Morris, W.; Leung, B.; Furukawa, H.; Yaghi, O. K.; He, N.; Hayashi, H.; Houndonougbo, Y.; Asta, M.; Laird, B. B.; Yaghi, O. M. *J. Am. Chem. Soc.* **2010**, *132*, 11006.

(14) Nouar, F.; Eckert, J.; Eubank, J. F.; Forster, P.; Eddaoudi, M. *J. Am. Chem. Soc.* **2009**, *131*, 2864.

(15) Spek, A. L. *J. Appl. Crystallogr.* **2003**, *36*, 7.




DOI: 10.1021/jacs.5b06929
*J. Am. Chem. Soc.* 2015, 137, 12203−12206